HAL
open science

From filamentary clouds to prestellar cores to the stellar IMF: Initial highlights from the Herschel Gould Belt survey

Ph. André, A. Men'Shchikov, Sylvain Bontemps, V. Könyves, F. Motte, N. Schneider, P. Didelon, V. Minier, P. Saraceno, D. Ward-Thompson, et al.

To cite this version:

Ph. André, A. Men'Shchikov, Sylvain Bontemps, V. Könyves, F. Motte, et al.. From filamentary clouds to prestellar cores to the stellar IMF: Initial highlights from the Herschel Gould Belt survey. Astronomy and Astrophysics - A&A, 2010, 518, pp.L102. 10.1051/0004-6361/201014666 . hal-00523064

HAL Id: hal-00523064

https://hal.science/hal-00523064v1

Submitted on 29 Oct 2020

HAL is a multi-disciplinary open access archive for the deposit and dissemination of scientific research documents, whether they are published or not. The documents may come from teaching and research institutions in France or abroad, or from public or private research centers.

L'archive ouverte pluridisciplinaire **HAL**, est destinée au dépôt et à la diffusion de documents scientifiques de niveau recherche, publiés ou non, émanant des établissements d'enseignement et de recherche français ou étrangers, des laboratoires publics ou privés.

Astronomy & Astrophysics manuscript no. herschel˙gb˙sdp˙aa
October 23, 2018
© ESO 2018

arXiv:1005.2618v2 [astro-ph.GA] 25 May 2010

Letter to the Editor

From filamentary clouds to prestellar cores to the stellar IMF: Initial highlights from the *Herschel*⋆ Gould belt survey⋆⋆

Ph. André[1], A. Men'shchikov[1], S. Bontemps[1], V. Könyves[1], F. Motte[1], N. Schneider[1], P. Didelon[1], V. Minier[1], P. Saraceno[5], D. Ward-Thompson[3], J. Di Francesco[10], G. White[18,22], S. Molinari[5], L. Testi[17], A. Abergel[2], M. Griffin[3], Th. Henning[11], P. Royer[7], B. Merín[13], R. Vavrek[13], M. Attard[1], D. Arzoumanian[1], C. D. Wilson[19], P. Ade[3], H. Aussel[1], J.-P. Baluteau[4], M. Benedettini[5], J.-Ph. Bernard[6], J.A.D.L. Blommaert[7], L. Cambrésy[8], P. Cox[9], A. Di Giorgio[5], P. Hargrave[3], M. Hennemann[1], M. Huang[12], J. Kirk[3], O. Krause[11], R. Launhardt[11], S. Leeks[18], J. Le Pennec[1], J.Z. Li[12], P. G. Martin[14], A. Maury[1], G. Olofsson[15], A. Omont[16], N. Peretto[1], S. Pezzuto[5], T. Prusti[21], H. Roussel[16], D. Russeil[4], M. Sauvage[1], B. Sibthorpe[20], A. Sicilia-Aguilar[11], L. Spinoglio[5], C. Waelkens[7], A. Woodcraft[20], and A. Zavagno[4]

(Affiliations can be found after the references)

Received 1 April 2010; accepted 4 May 2010

ABSTRACT

We summarize the first results from the Gould belt survey, obtained toward the Aquila Rift and Polaris Flare regions during the 'science demonstration phase' of *Herschel*. Our 70–500 μm images taken in parallel mode with the SPIRE and PACS cameras reveal a wealth of filamentary structure, as well as numerous dense cores embedded in the filaments. Between ∼ 350 and 500 prestellar cores and ∼ 45–60 Class 0 protostars can be identified in the Aquila field, while ∼ 300 unbound starless cores and no protostars are observed in the Polaris field. The prestellar core mass function (CMF) derived for the Aquila region bears a strong resemblance to the stellar initial mass function (IMF), already confirming the close connection between the CMF and the IMF with much better statistics than earlier studies. Comparing and contrasting our *Herschel* results in Aquila and Polaris, we propose an observationally-driven scenario for core formation according to which complex networks of long, thin filaments form first within molecular clouds, and then the densest filaments fragment into a number of prestellar cores via gravitational instability.

Key words. stars: formation – stars: luminosity function, mass function – stars: protostars – ISM: clouds – ISM: structure – submillimeter: ISM

1. Introduction

The *Herschel* Space Observatory (Pilbratt et al. 2010) offers a unique opportunity to improve our global understanding of the earliest phases of star formation. Here, we present first highlights from the Gould belt survey, one of the largest key projects with *Herschel* (cf. André & Saraceno 2005), based on extensive far-infrared and submillimeter mapping of nearby molecular clouds with both the SPIRE (Griffin et al. 2010) and PACS (Poglitsch et al. 2010) bolometer cameras. This SPIRE/PACS imaging survey will cover the bulk of the nearest ($d \leq 0.5$ kpc) cloud complexes in the Galaxy, which are mostly located in the Gould belt, a giant (∼ 700 pc × 1000 pc), flat structure inclined by ∼ 20° to the Galactic plane (e.g., Guillout 2001). Since the ∼ 15″ angular resolution of *Herschel* around $\lambda \sim 200\,\mu$m is adequate for probing individual (∼ 0.01–0.1 pc) star-forming cores up to ∼ 0.5 kpc away, the cloud complexes of the Gould belt correspond to the volume of Galactic space where *Herschel* imaging can be best used to characterize in detail the earliest stages of star formation.

The immediate observational objective of the Gould belt survey is to obtain complete samples of nearby prestellar cores and Class 0 protostars with well characterized luminosities, temperatures, and density profiles, as well as robust core mass functions and protostar luminosity functions, in a variety of star-forming environments. An order of magnitude more cold prestellar cores than already identified from the ground are expected to be found in the entire survey, which should allow us to derive an accurate prestellar core mass function (CMF) from the pre-brown-dwarf to the intermediate-mass range. Thanks to its high sensitivity and large spatial dynamic range, this *Herschel* survey can also probe, for the first time, the link between low-density cirrus-like structures in the interstellar medium (ISM) and compact self-gravitating cores. The main scientific goal is to elucidate the physical mechanisms responsible for the formation of prestellar cores out of the diffuse ISM, which is crucial for understanding the origin of the stellar initial mass function (IMF).

Our first results, obtained toward the Aquila Rift and Polaris clouds, are very promising (e.g., Könyves et al. 2010, Bontemps et al. 2010, Men'shchikov et al. 2010, Ward-Thompson et al. 2010, and Miville-Deschênes et al. 2010). As discussed in Sect. 4 of this paper, they suggest that prestellar cores result from the *gravitational fragmentation of filaments* in the cold ISM.

2. *Herschel* observations

The *Herschel* survey was designed to cover the densest portions of the Gould belt with SPIRE at 250–500 μm and PACS at 100–160 μm. The observational goal is to make a complete, homogeneous mapping of the $A_V > 3$ regions with SPIRE and the $A_V > 6$ regions with PACS, and representative areas at $A_V \sim 1$–3

Send offprint requests to: pandre@cea.fr

⋆ *Herschel* is an ESA space observatory with science instruments provided by European-led Principal Investigator consortia and with important participation from NASA.

⋆⋆ Appendix A and Figs. 3, 4 are only available in electronic form via http://www.edpsciences.org

levels with both instruments. The survey sensitivity (better than $A_V \sim 1$ at the 5σ level) will allow us to probe the structure of nearby molecular clouds *down to the level of the interface with their atomic gas envelopes*. The 15 target clouds span a range of physical conditions, from active, cluster-forming complexes to quiescent regions with lower or no star formation activity[1].

Our *Herschel* mapping consists of two steps:

(1) A wide-field SPIRE/PACS survey of a total surface area $\sim 160\,\mathrm{deg}^2$ using the so-called "parallel mode" with a scanning speed of 60″/s and the PACS 70 μm and 160 μm bands. In this first step, the main goal is to acquire adequate SPIRE 250–500 μm data for all of the target regions. The PACS data acquired simultaneously yield very useful information at 70 μm and 160 μm through most of the SPIRE survey, but do not have optimal (diffraction-limited) angular resolution. We selected the 70 μm filter for the blue band of PACS to obtain a good diagnostic of the presence of embedded protostars (cf. Dunham et al. 2008) throughout the mapped regions.

(2) A dedicated PACS-only survey of a total surface area $\sim 65\,\mathrm{deg}^2$, observing the 100 μm and 160 μm bands with a scanning speed of 20″/s. This second step is supposed to provide data of optimal sensitivity and resolution at 100 μm and 160 μm.

The Aquila Rift and Polaris flare regions were observed in parallel mode with both SPIRE and PACS (step 1) during the science demonstration phase of *Herschel*. The corresponding observations are described in detail by Könyves et al. (2010), Bontemps et al. (2010), Men'shchikov et al. (2010), and Ward-Thompson et al. (2010) in this special A&A issue. The Polaris flare field is a high-latitude *translucent* cloud with little to no star formation at $d \sim 150$ pc (e.g., Heithausen et al. 2002), and is expected to have the *lowest level of background cloud emission and cirrus confusion noise* in the entire Gould belt survey. At the other extreme, the Aquila field is a very active star-forming complex at $d \sim 260$ pc (e.g., Gutermuth et al. 2008), and is expected to have the *highest level of background cloud emission and cirrus confusion noise* in the whole survey. Sensitive Galactic far-IR imaging surveys such as the one discussed here are not limited by instrumental sensitivity but by confusion arising from small-scale cirrus/cloud structure (cf. Roy et al. 2010 and references therein). The levels of background cloud fluctuations observed in the Aquila and Polaris fields allow us to roughly estimate the whole range of cirrus confusion noise levels that will affect the Gould belt survey. In the Aquila field, the observed rms level of cirrus or "structure" noise (as measured on the typical scales of dense cores) ranges from ~ 30 mJy/18″-beam to ~ 300 mJy/18″-beam at $\lambda = 250\,\mu$m, which is a factor of ~ 3–30 above the rms instrumental noise. In contrast, in the Polaris field, the rms level of emission fluctuations measured in the SPIRE 250 μm map is only ~ 10–30 mJy/18″-beam, which is very close to the rms sensitivity level expected after two cross-scans in parallel mode at 60″/s. Assuming the dust opacity of Hildebrand (1983) and the median dust temperatures derived from our *Herschel* maps, the above surface-brightness sensitivity levels translate into 5σ column-density detection thresholds of $N_{\mathrm{H2}} \lesssim 3 \times 10^{20}\,\mathrm{cm}^{-2}$ in Polaris and $N_{\mathrm{H2}} \lesssim 10^{21}\,\mathrm{cm}^{-2}$ in Aquila (in agreement with the column-density maps shown by Ward-Thompson et al. 2010 and Könyves et al. 2010). This high column-density sensitivity, coupled with the unprecedented surface brightness and spatial dynamic ranges of our *Herschel* mapping, allows us to probe, for the first time, the physical connection between the structure of the diffuse ISM and the formation of prestellar cores (cf. Sect. 4).

[1] See http://gouldbelt-herschel.cea.fr/ for the list of target fields.

The corresponding mass sensitivities for typical prestellar/protostellar cores are $\sim 0.3\,M_\odot$ (85% completeness level) in Aquila ($d = 260$ pc) and $\sim 0.01\,M_\odot$ (85% completeness level) in Polaris ($d = 150$ pc). These completeness numbers were estimated by performing Monte-Carlo simulations as described by Könyves et al. (2010) in the case of Aquila. The initial results obtained in Aquila and Polaris therefore confirm that the completeness level of our *Herschel* census for prestellar cores will reach the pre-brown dwarf mass regime ($M_{\mathrm{core}} < 0.08\,M_\odot$) in the nearest molecular clouds ($d \sim 150$ pc) of the Gould belt.

3. Main results and analysis

The *Herschel* images of the Aquila Rift and Polaris flare regions exhibit extensive filamentary structure, as well as numerous dense cores situated along these filaments (see Fig. 1, online Fig. 3, and Men'shchikov et al. 2010). A total of 541 starless cores (~ 0.01–0.1 pc in size) can be identified in the whole ($\gtrsim 3.3^\circ \times 3.3^\circ$) Aquila field, most ($> 60\%$) of which appear to be self-gravitating and prestellar in nature. The latter is inferred from: (1) a comparison of the core masses derived from the SPIRE/PACS spectral energy distributions with local values of the Jeans or Bonnor-Ebert (BE) mass also estimated from *Herschel* data (see Könyves et al. 2010); (2) the positions of the cores in a mass versus size diagram (cf. online Fig. 4), which are close to the loci expected for critical isothermal BE spheres at gas temperatures ~ 7–20 K; and (3) the mean column densities of the cores, which exceed the background column densities by a median factor ~ 1.5 as expected for critically self-gravitating BE spheres. The shape of the core mass function (CMF) derived for this sample of Aquila cores closely resembles the IMF (Fig. 2–left – see Könyves et al. 2010 for the CMF of the Aquila central region and Appendix A for details on the derivation of core masses). In contrast, the 302 starless cores identified in the cirrus-like Polaris cloud with the same clump-finding algorithm (*getsources* – see Men'shchikov et al. 2010) appear to be mostly unbound (cf. online Fig. 4) and their mass distribution does *not* follow the IMF, with a peak at an order of magnitude smaller mass (Fig. 2–right). Only 5 of the Polaris cores are reasonably close to being gravitationally bound and thus possibly prestellar in nature (see Ward-Thompson et al. 2010). Between 45 and 60 Class 0 protostars are revealed by *Herschel* in the Aquila field (Bontemps et al. 2010), while not a single protostar is detected in the Polaris region.

The Aquila filaments harboring embedded protostars and/or large concentrations of prestellar cores are all characterized by higher column densities ($N_{\mathrm{H_2}} \gtrsim 10^{22}\,\mathrm{cm}^{-2}$), suggesting that they are gravitationally unstable (see Fig. 1–left). In contrast, both the Polaris filaments and the quiescent, non-star-forming filaments observed in Aquila have much lower column densities (up to a few $10^{21}\,\mathrm{cm}^{-2}$), suggesting they are gravitationally stable (see Fig. 1–right and Sect. 4 below).

4. Discussion and conclusions

The *Herschel* early results obtained toward the Aquila star-forming complex confirm that the prestellar CMF resembles the stellar IMF, using data with already a factor of ~ 2 to 9 better counting statistics than earlier (sub)-millimeter continuum or near-IR extinction surveys (e.g., Motte et al. 1998, Johnstone et al. 2000, Enoch et al. 2006, Stanke et al. 2006, Nutter & Ward-Thompson 2007, Alves et al. 2007). The close resemblance between the Aquila CMF and the IMF in both shape and

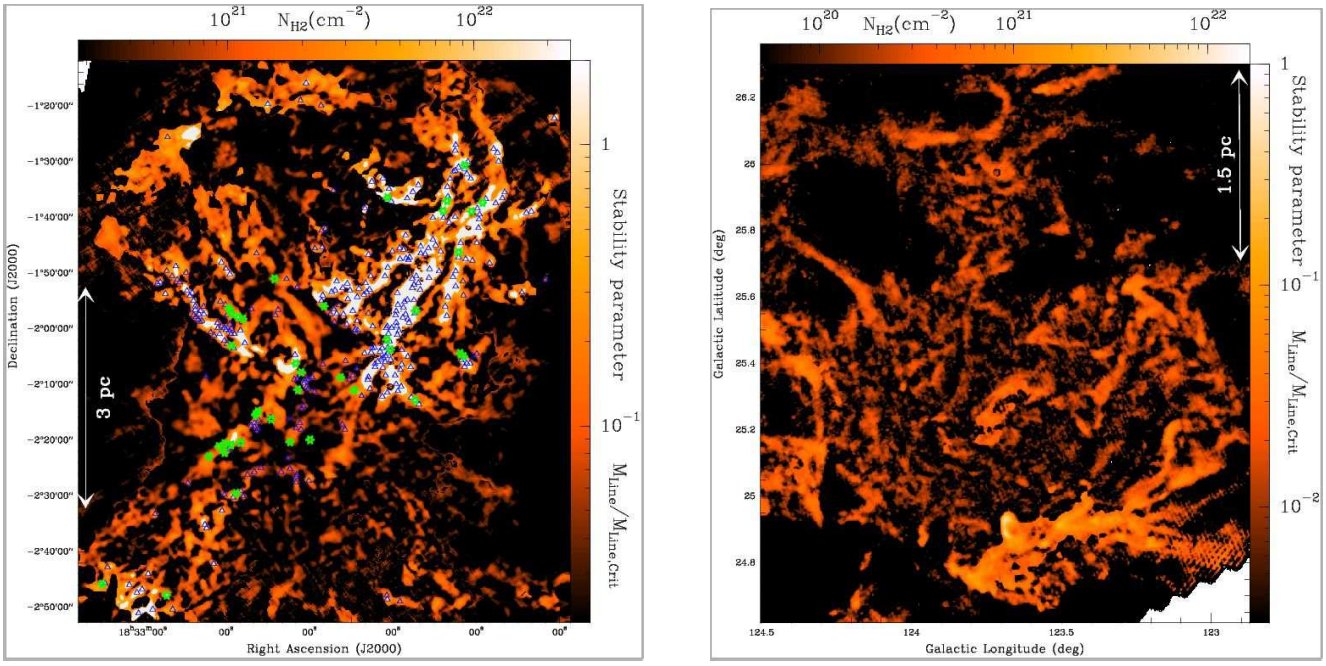

Fig. 1. Column density maps of two subfields in Aquila (left) and Polaris (right) derived from our SPIRE/PACS data. The contrast of the filaments with respect to the non-filamentary background has been enhanced using a curvelet transform as described in Appendix A. Given the typical width ~ 10000 AU of the filaments, these column density maps are equivalent to *maps of the mass per unit length along the filaments*. The color scale shown on the right of each panel is given in approximate units of the critical line mass of Inutsuka & Miyama (1997) as discussed in Sect. 4. The areas where the filaments have a mass per unit length larger than half the critical value and are thus likely gravitationally unstable have been highlighted in white. The maximum line mass observed in the Polaris region is only ~ 0.45 × the critical value, suggesting that the Polaris filaments are stable and unable to form stars at the present time. The candidate Class 0 protostars and bound prestellar cores identified in Aquila by Bontemps et al. (2010) and Könyves et al. (2010) are shown as green stars and blue triangles, respectively. Note the good correspondence between the spatial distribution of the bound cores/protostars and the regions where the filaments are unstable to gravitational collapse.

mass scale suggests that, as a class, the self-gravitating prestellar cores identified in far-IR/submilimeter continuum imaging studies such as the present *Herschel* survey may form stars on a one-to-one basis, with a fixed and relatively high local efficiency, i.e., $\epsilon_{\rm core} \equiv M_\star/M_{\rm core} \sim 20-40\%$ in Aquila. This is consistent with theoretical models according to which the stellar IMF is in large part determined by pre-collapse cloud fragmentation, prior to the protostellar accretion phase (cf. Larson 1985; Padoan & Nordlund 2002; Hennebelle & Chabrier 2008). There are several caveats to this simple picture (cf. discussion in André et al. 2009), and detailed analysis of the data from the whole Gould belt survey will be required to fully characterize the CMF–IMF relationship and, e.g., investigate possible variations in the efficiency $\epsilon_{\rm core}$ with environment. It is nevertheless already clear that one of the keys to the problem of the origin of the IMF lies in a good understanding of the formation process of prestellar cores, even if additional processes, such as rotational subfragmentation of prestellar cores into binary/multiple systems (e.g., Bate et al. 2003), probably also play an important role.

Our *Herschel* initial results also provide *key insight into the core formation issue*. They support an emerging picture (see also Myers 2009) according to which complex networks of long, thin filaments form first within molecular clouds, possibly as a result of interstellar MHD turbulence, and then the densest filaments fragment into a number of prestellar cores via gravitational instability. That the formation of filaments in the diffuse ISM represents the first step toward core/star formation is suggested by the filaments *already* being omnipresent in a diffuse, non-star-forming cloud such as Polaris (cf. Fig. 1–right, Men'shchikov et al. 2010, and Miville-Deschênes et al. 2010). The second step appears to be the gravitational fragmentation of a subset of the filaments into self-gravitating cores. This observationally-driven scenario can be placed on a stronger footing by comparing our *Herschel* results to existing models of filamentary cloud fragmentation. Inutsuka & Miyama (1992, 1997) showed that an unmagnetized isothermal filament is unstable to axisymmetric perturbations if the line mass or mass per unit length, $M_{\rm line}$, of the filament is larger than the critical value required for equilibrium, $M_{\rm line,crit}^{\rm unmag} = 2\,c_s^2/G$, where c_s is the isothermal sound speed. Remarkably, the critical line mass only depends on gas temperature (Ostriker 1964) and is modified by only a factor of order unity for filaments with realistic levels of magnetization (Fiege & Pudritz 2000). Figure 1 shows maps of the mass per unit length, expressed in approximate units of the critical line mass, for the filaments detected by *Herschel* in Aquila and Polaris. These maps were constructed from the column density maps derived from our SPIRE/PACS images (see Appendix A) by multiplying the local column density of the filaments by their measured typical width (FWHM ~ 14000 AU in Aquila and ~ 9000 AU in Polaris, before deconvolution – cf. Men'shchikov et al. 2010). In Fig. 1, the critical line mass corresponding to a gas temperature of 10 K ($M_{\rm line,crit}^{\rm 10K,unmag} \approx 15\,M_\odot$/pc) was adopted throughout the fields, but nearly identical results are obtained if the dust temperature maps derived from the *Herschel* images (cf. Bontemps et al. 2010) are used instead. The results (cf. Fig. 1) show that most (> 60%) of the bound prestellar cores identified in Aquila are concentrated in *supercritical* filaments with $M_{\rm line} > M_{\rm line,crit}^{\rm unmag}$. Furthermore, virtually all supercritical fil-

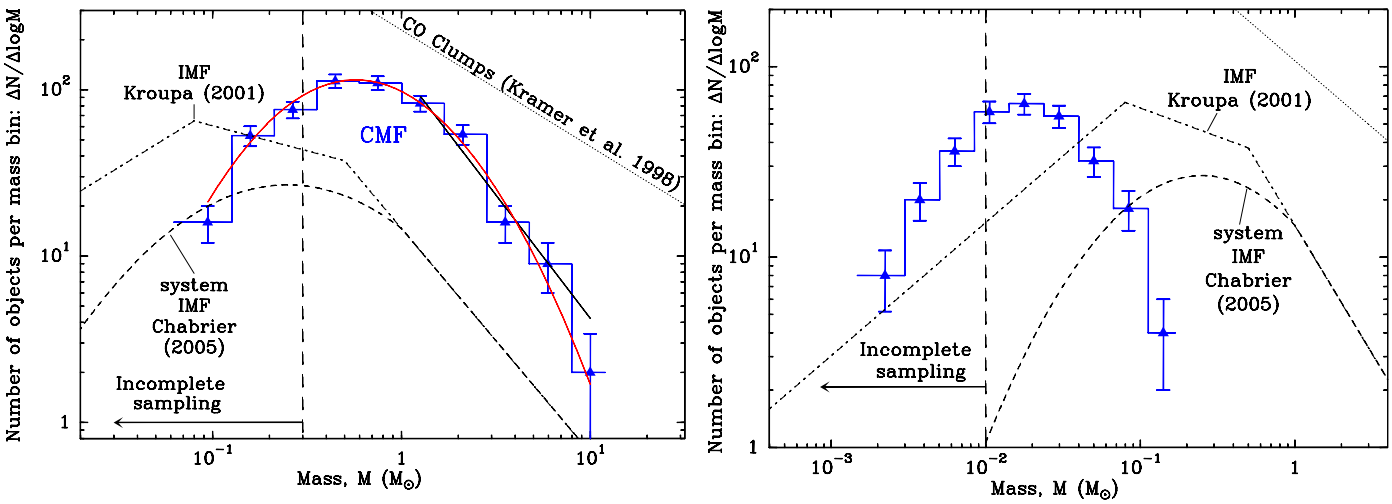

Fig. 2. Core mass functions (blue histograms with error bars) derived from our SPIRE/PACS observations of the Aquila (left) and Polaris (right) regions, which reveal of total of 541 candidate prestellar cores and 302 starless cores, respectively. A lognormal fit (red curve) and a power-law fit (black solid line) to the high-mass end of the Aquila CMF are superimposed in the left panel. The power-law fit has a slope of -1.5 ± 0.2 (compared to a Salpeter slope of -1.35 in this $dN/d\log M$ format), while the lognormal fit peaks at $\sim 0.6\,M_\odot$ and has a standard deviation of ~ 0.43 in $\log_{10}M$. The IMF of single stars (corrected for binaries – e.g., Kroupa 2001), the IMF of multiple systems (e.g., Chabrier 2005), and the typical mass spectrum of CO clumps (e.g., Kramer et al. 1998) are also shown for comparison. Note the remarkable similarity between the Aquila CMF and the stellar IMF, suggesting a ~ one-to-one correspondence between core mass and star/system mass with $M_{\star\rm sys} = \epsilon M_{\rm core}$ and $\epsilon \approx 0.4$ in Aquila.

aments harbor prestellar cores and/or embedded protostars, in agreement with the view that they are collapsing and actively forming stars at the present time. In particular, this is the case for the Aquila main filament, which has $M_{\rm line} > 5 \times M_{\rm line,crit}^{\rm unmag}$ and is associated with a very rich protocluster (Serpens South – see Gutermuth et al. 2008, Bontemps et al. 2010). In contrast, the *subcritical* filaments with $M_{\rm line} < M_{\rm line,crit}^{\rm unmag}$ are generally devoid of prestellar cores and protostars, which is consistent with the view that they are gravitationally stable, hence neither collapsing nor forming stars. *All* of the Polaris filaments appear to be in the subcritical regime, the maximum observed value of the stability parameter being $M_{\rm line}/M_{\rm line,crit}^{\rm unmag} \sim 0.45$, and it is unclear whether they will evolve into the unstable regime or not.

It is noteworthy that the critical line mass approximately corresponds to a critical column density $N_{\rm H_2,crit} \sim 10^{22}$ cm^{-2}, i.e., to a critical visual extinction $A_{\rm V,crit} \sim 10$. Our *Herschel* findings thus provide an *explanation* of the visual extinction threshold for core formation found by earlier ground-based studies (e.g., Onishi et al. 1998, Johnstone et al. 2004). Prestellar cores are only observed above a threshold $A_{\rm V,crit}$ because they form out of a filamentary background and only the supercritical, gravitationally unstable filaments are able to fragment into bound cores.

Confirming and refining this scenario for core formation will require the results of the entire *Herschel* survey, as well as follow-up (sub-)millimeter dust polarimetry and molecular line observations to, e.g., clarify the roles of magnetic fields, turbulence, and gravity in forming the filaments. Our initial results are nevertheless extremely encouraging. Extrapolating from the $\gtrsim$ 500 prestellar cores and $\gtrsim$ 45 Class 0 protostars identified in the ~ 19 deg^2 covered by the Aquila and Polaris fields, we expect that the ~ 160 deg^2 Gould belt survey will reveal a total of about 4500 prestellar cores, including a large number of candidate pre-brown dwarfs in the nearest ($d \sim 150$ pc) clouds, and more than 350 Class 0 protostars. This will provide a unique database, including the southern hemisphere, for follow-up high-resolution molecular line/dust continuum studies of the physics of individual cores and protostars with ALMA.

Acknowledgements. SPIRE has been developed by a consortium of institutes led by Cardiff Univ. (UK) and including Univ. Lethbridge (Canada); NAOC (China); CEA, LAM (France); IFSI, Univ. Padua (Italy); IAC (Spain); Stockholm Observatory (Sweden); Imperial College London, RAL, UCL-MSSL, UKATC, Univ. Sussex (UK); Caltech, JPL, NHSC, Univ. Colorado (USA). This development has been supported by national funding agencies: CSA (Canada); NAOC (China); CEA, CNES, CNRS (France); ASI (Italy); MCINN (Spain); SNSB (Sweden); STFC (UK); and NASA (USA). PACS has been developed by a consortium of institutes led by MPE (Germany) and including UVIE (Austria); KU Leuven, CSL, IMEC (Belgium); CEA, LAM (France); MPIA (Germany); INAF-IFSI/OAA/OAP/OAT, LENS, SISSA (Italy); IAC (Spain). This development has been supported by the funding agencies BMVIT (Austria), ESA-PRODEX (Belgium), CEA/CNES (France), DLR (Germany), ASI/INAF (Italy), and CICYT/MCYT (Spain).

References

Alves, J. F., Lombardi, M., & Lada, C. J. 2007, A&A, 462, L17
André, P., Basu, S., & Inutsuka, S.-I. 2009, in Structure Formation in Astrophysics, Ed. G. Chabrier, Cambridge University Press, p. 254
André, P. , & Saraceno, P. 2005, in The Dusty and Molecular Universe: A Prelude to *Herschel* and ALMA, ESA SP-577, p. 179
Bate, M. R., Bonnell, I. A., & Bromm, V. 2003, MNRAS, 339, 577
Bontemps, S., André, Ph., Könyves, V. et al. 2010, A&A, this volume
Chabrier, G. 2005, in The Initial Mass Function 50 years later, Eds. E. Corbelli et al., p.41
Dunham, M.M., Crapsi, A., Evans, N.J. et al. 2008, ApJS, 179, 249
Elmegreen, B.G., & Falgarone, E. 1996, ApJ, 471, 816
Enoch, M. L., Young, K. E., Glenn, J., Evans, N. J. et al. 2006, ApJ, 638, 293
Fiege, J.D., & Pudritz, R.E. 2000, MNRAS, 311, 85
Griffin, M., Abergel, A., Abreu, A. et al. 2010, A&A, this volume
Guillout, P. 2001, in From Darkness to Light, Eds. T. Montmerle & P. André, ASP Conf. Ser., 243, p. 677
Gutermuth, R.A., Bourke, T.L., Allen, L.E. et al. 2008, ApJ, 673, L151
Heithausen, A. et al. 2002, A&A, 383, 591
Hennebelle, P., & Chabrier, G. 2008, ApJ, 684, 395
Hildebrand, R.H. 1983, QJRAS, 24, 267
Inutsuka, S-I, & Miyama, S.M. 1992, ApJ, 388, 392
Inutsuka, S-I, & Miyama, S.M. 1997, ApJ, 480, 681
Johnstone, D., Wilson, C.D., Moriarty-Schieven, G. et al. 2000, ApJ, 545, 327
Johnstone, D., Di Francesco, J., & Kirk, H. 2004, ApJ, 611, L45

Könyves, V., André, Ph., Men'shchikov, A. et al. 2010, A&A, this volume
Kramer, C., Stutzki, J., Rohrig, R., Corneliussen, U. 1998, A&A, 329, 249
Kroupa, P. 2001, MNRAS, 322, 231
Larson, R. 1985, MNRAS, 214, 379
Men'shchikov, A., André, Ph., Didelon, P. et al. 2010, A&A, this volume
Miville-Deschênes, M.-A., Martin, P.G., Abergel, A. et al. 2010, A&A, this volume
Motte, F., André, P., & Neri, R. 1998, A&A, 365, 440
Motte, F., André, P., Ward-Thompson, D., & Bontemps, S. 2001, A&A, 372, L41
Myers, P.C. 2009, ApJ, 700, 1609
Nutter, D., & Ward-Thompson, D. 2007, MNRAS, 374, 1413
Onishi, T., Mizuno, A., Kawamura, A. et al. 1998, ApJ, 502, 296
Ostriker, J. 1964, ApJ, 140, 1056
Padoan, P. & Nordlund, A. 2002, ApJ, 576, 870
Pilbratt, G.L., Riedinger, J.R., Passvogel, T. et al. 2010, A&A, this volume
Poglitsch, A., Waelkens, C., Geis, N. et al. 2010, A&A, this volume
Roy, A., Ade, P.A.R., Bock, J.J. et al. 2010, ApJ, 708, 1611
Stanke, T., Smith, M. D., Gredel, R., & Khanzadyan, T. 2006, A&A, 447, 609
Starck, J. L., Donoho, D. L., Candès, E. J. 2003, A&A, 398, 785
Ward-Thompson, D., Kirk, J.M., André, P. et al. 2010, A&A, this volume

---

[1] Laboratoire AIM, CEA/DSM–CNRS–Université Paris Diderot, IRFU/Service d'Astrophysique, CEA Saclay, 91191 Gif-sur-Yvette, France
[2] Institut d'Astrophysique Spatiale, CNRS/Université Paris-Sud 11, 91405 Orsay, France
[3] School of Physics and Astronomy, Cardiff University, Queens Buildings, The Parade, Cardiff CF243AA, UK
[4] Laboratoire dAstrophysique de Marseille , CNRS/INSU - Université de Provence, 13388 Marseille cedex 13, France
[5] INAF-Istituto Fisica Spazio Interplanetario, Via Fosso del Cavaliere 100, I-00133 Roma, Italy
[6] CESR, Observatoire Midi-Pyrénées (CNRS-UPS), Université de Toulouse, BP 44346, 31028 Toulouse Cedex 04, France
[7] Instituut voor Sterrenkunde, K.U.Leuven, Celestijnenlaan 200D, B-3001 Leuven, Belgium
[8] CDS, Observatoire de Strasbourg, 11, rue de l'Université, 67000 Strasbourg, France
[9] IRAM, 300 rue de la Piscine, Domaine Universitaire, 38406 Saint Martin d'Hères, France
[10] National Research Council of Canada, Herzberg Institute of Astrophysics, Victoria, BC, V9E 2E7, Canada
[11] Max-Planck-Institut für Astronomie, Königstuhl 17, D-69117 Heidelberg, Germany
[12] National Astronomical Observatories, Chinese Academy of Sciences, Beijing 100012, China
[13] Herschel Science Centre, ESAC, ESA, PO Box 78, Villanueva de la Cañada, 28691 Madrid, Spain
[14] Canadian Institute for Theoretical Astrophysics, University of Toronto, 60 St. George Street, Toronto, ONM5S3H8, Canada
[15] Stockholm Observatory, AlbaNova University Center, Roslagstullsbacken 21, SE-106 91 Stockholm, Sweden
[16] Institut d'Astrophysique de Paris, Université Pierre & Marie Curie, 98 bis Boulevard Arago, 75014 Paris, France
[17] INAF, Osservatorio Astrofisico di Arcetri, Firenze, Italy
[18] Space Science and Technology Department, Rutherford Appleton Laboratory, Chilton, Didcot, Oxon OX11 0QX, UK
[19] Dept. of Physics & Astronomy, McMaster University, Hamilton, Ontario, L8S 4M1, Canada
[20] UK Astronomy Technology Centre, Royal Observatory Edinburgh, Blackford Hill, EH9 3HJ, UK
[21] ESA/ESTEC, P.O. Box 299, 2200 AG Noordwijk, The Netherlands
[22] Department of Physics & Astronomy, The Open University, Milton Keynes MK7 6AA, UK

Appendix A: Derivation of core/filament properties and effects of distance uncertainties

As described in more detail in a companion paper by Könyves et al. (2010) on Aquila, the masses of the cores identified in the *Herschel* images with the *getsources* algorithm (see Men'shchikov et al. 2010) were derived by fitting greybody functions to the spectral energy distributions (SEDs) constructed from the integrated flux densities measured with SPIRE/PACS for each core. We assumed the dust opacity law $\kappa_\nu = 0.1\ (\nu/1000\ \mathrm{GHz})^2\ \mathrm{cm}^2/\mathrm{g}$, where ν denotes frequency and κ_ν is the dust opacity per unit (gas + dust) mass column density. This dust opacity law, which is very similar to that advocated by Hildebrand (1983), is consistent with the value $\kappa_{1.3\mathrm{mm}} = 0.005\ \mathrm{cm}^2/\mathrm{g}$ adopted for starless cores in numerous earlier studies (e.g., Motte et al. 1998). Ignoring any systematic distance effect (see below), the core mass uncertainties are dominated by the uncertainty in κ_ν, typically a factor of ~ 2. Cores were classified as either protostellar or starless based on the presence or absence of significant PACS emission at 70 μm, respectively (cf. Bontemps et al. 2010 and Dunham et al. 2008). In the Polaris field, the cirrus noise level is so low (cf. Fig. 4–right) that we cannot exclude that a fraction of the 302 candidate starless cores extracted with *getsources* correspond to background galaxies.

A column density map was derived for each region from the *Herschel* images smoothed to the SPIRE 500 μm resolution (36.9″ FWHM) using a similar SED fitting procedure on a pixel by pixel basis (see, e.g., Figs. 1 and 6 of Könyves et al. 2010 for Aquila). To obtain the maps of the filamentary background shown in Fig. 1 of this paper, we then performed a "morphological component analysis" decomposition (e.g., Starck et al. 2003) of the original column density maps on curvelets and wavelets. The curvelet component images shown in Fig. 1 provide a good measurement of the column density distribution of the filamentary background after subtraction of the compact sources/cores since the latter are contained in the wavelet component. We estimate that these column density maps are accurate to within a factor of ~ 2. The scaling in terms of the mass per unit length along the filaments is more uncertain, however, as it depends on distance (see below) and would in principle require a detailed analysis of the radial profiles of the filaments, which is beyond the scope of the present letter. Here, we simply assumed that the filaments had a Gaussian radial column density profile and multiplied the surface density maps by $\sqrt{\frac{2\pi}{8\ln 2}} \times W \approx 1.06\,W$, where W is the typical FWHM width of the filaments. We assumed a mean molecular weight of $\mu = 2.33$. At this stage, the correspondence between the critical line mass of the filaments, $M^{\mathrm{unmag}}_{\mathrm{line,crit}}$, and the visual extinction threshold, $A_{\mathrm{V,crit}} \sim 10$ (see Sect. 4), is thus accurate to at best a factor of $\gtrsim 2$.

There is some ambiguity concerning the distance to the Aquila Rift region. A number of arguments, presented in a companion paper by Bontemps et al. (2010), suggest that the whole region corresponds to a coherent cloud complex at $d_- = 260$ pc (see also Gutermuth et al. 2008), which is the default distance adopted in the present paper for Aquila. However, other studies in the literature (see references in Bontemps et al. 2010) place the complex at a larger distance, $d_+ = 400$ pc. It is thus worth discussing briefly how our Aquila results would be affected if we adopted the larger distance estimate, d_+, instead of d_-. The core mass estimates, which scale as $S_\nu\, d^2/[B_\nu(T_\mathrm{d})\,\kappa_\nu]$ where S_ν is integrated flux density and $B_\nu(T_\mathrm{d})$ is the Planck function, would systematically increase by a factor of 2.4. This would shift the CMF shown in Fig. 2–left to the right and thus lower the efficiency ϵ_{core} from $\sim$ 20–40% to $\sim$ 10–20%. In the mass versus size diagram of Fig. 4, the cores would move upward as indicated in the left panel of the figure, which would *increase* the fraction of candidate bound cores in Aquila from 63% to 81%. The column density map of the Aquila filaments shown in Fig. 1 would be unchanged, but the scaling in terms of the mass per unit length along the filaments would change by $\sim$ 50% upward, since the physical width of the filaments would increase by $\sim$ 50%. In other words, the highlighted regions in Fig. 1–left, where the mass per unit length of the filaments exceeds half the critical value, would slightly *expand*, increasing the contrast with the Polaris filaments and improving the correspondence between the spatial distribution of the prestellar cores/protostars in Aquila and that of the gravitationally unstable filaments. To summarize, our main conclusions do not depend strongly on the adopted distance.

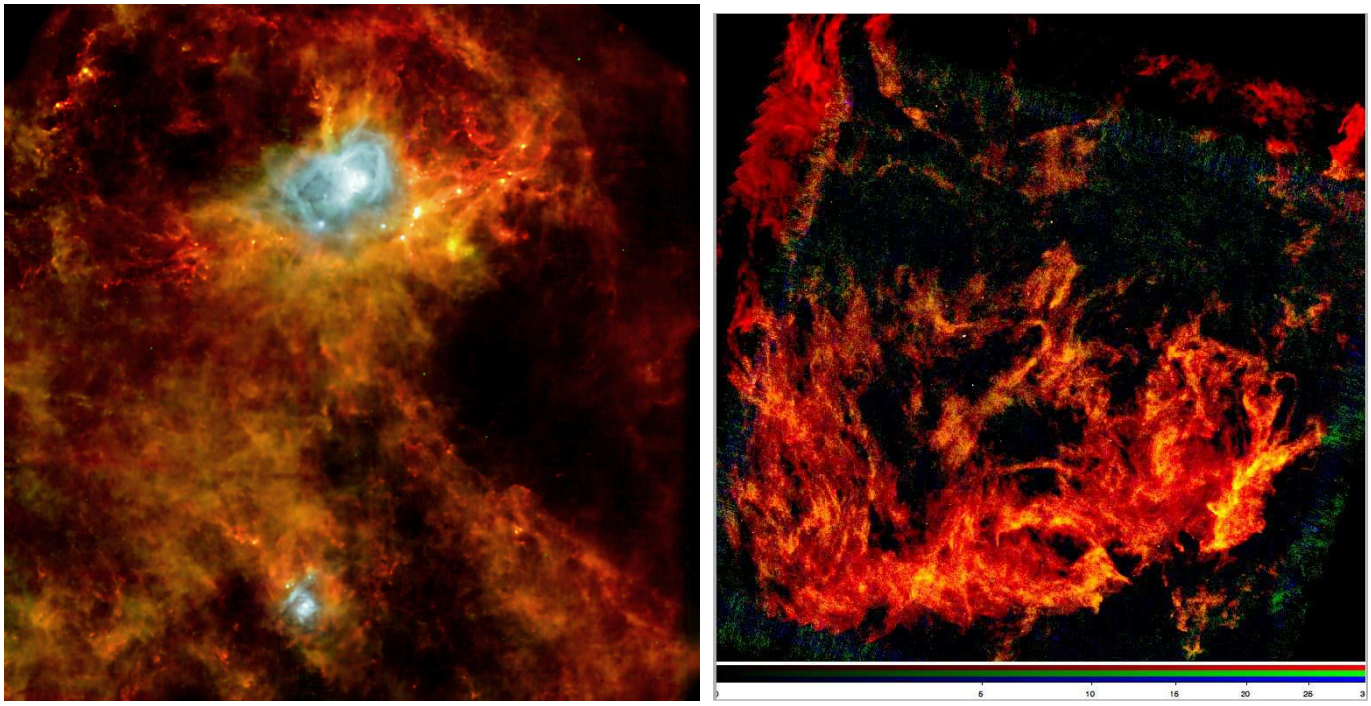

Fig. 3. Composite 3-color images of the ~ 11 deg^2 Aquila field (*left*) and the ~ 8 deg^2 Polaris field (*right*) produced from our PACS/SPIRE parallel-mode images at 70, 160, and 500 μm. The color coding of the Aquila image is such that Red = SPIRE 500 μm, Green = PACS 160 μm, Blue = PACS 70 μm. For the Polaris image, Red = combination of the three SPIRE bands, Green = PACS 160 μm, Blue = PACS 70 μm. The Aquila composite image was also the first release of "OSHI", ESA's Online Showcase of *Herschel* Images (cf. http://oshi.esa.int and http://www.esa.int/SPECIALS/Herschel/SEMT0T9K73G_0.html).

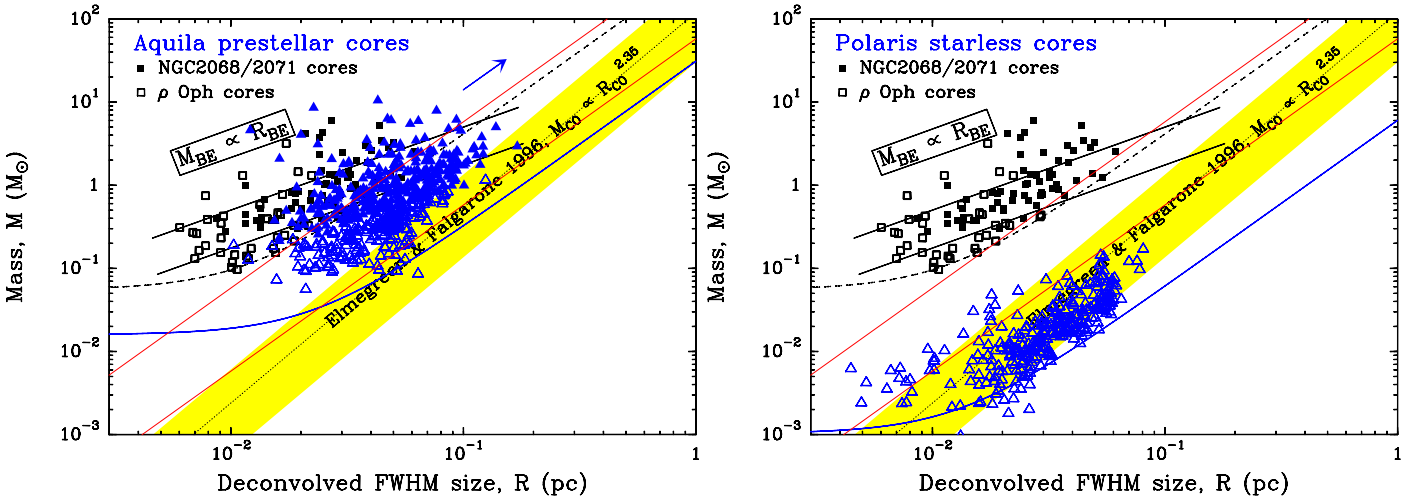

Fig. 4. Mass vs. size diagrams for the starless cores detected with *Herschel*-SPIRE/PACS in Aquila (left) and Polaris (right) (blue triangles). The masses were derived as explained in Appendix A (see also Könyves et al. 2010) and the sizes were measured at 250 μm. For reference, the locations of the (sub)mm continuum prestellar cores identified by Motte et al. (1998, 2001) in ρ Oph and NGC2068/2071, respectively, are shown, along with the correlation observed for diffuse CO clumps (shaded band – cf. Elmegreen & Falgarone 1996). The two black solid lines mark the loci of critically self-gravitating isothermal Bonnor-Ebert spheres at $T = 7$ K and $T = 20$ K, respectively. The 341 cores classified as prestellar by Könyves et al. (2010), out of a total of 541 starless cores in Aquila, are shown as filled triangles in the left panel. The 302 starless cores of Polaris lie much below the two Bonnor-Ebert lines in the right panel, suggesting they all are unbound. The red solid lines are two lines of constant mean column density at $N_{H_2} = 10^{21}$ cm^{-2} and $N_{H_2} = 10^{22}$ cm^{-2}, respectively. The 5σ detection threshold at $d = 150$ pc of existing ground-based (sub)mm (e.g., SCUBA) surveys as a function of size is shown by the dashed curve. (The shape of this curve reflects a constant sensitivity to column density until source size approaches the beam size.) The 5σ detection thresholds of our SPIRE 250 μm observations, given the estimated levels of cirrus noise (cf. Sect. 2) and assumed distances of 260 pc for Aquila and 150 pc for Polaris, are shown by the blue curves. The blue arrow in the left panel indicates how the positions of the *Herschel* cores (and the blue curve marking the detection threshold) would move in the diagram if a distance of 400 pc were adopted for Aquila instead of 260 pc (see Appendix A).